Activity of the MAP kinase ERK2 is controlled by a flexible surface loop

Jiandong Zhang[1], Faming Zhang[1], Douglas Ebert[2], Melanie H Cobb[2] and Elizabeth J Goldsmith[1]*

Departments of [1]Biochemistry and [2]Pharmacology, The University of Texas Southwestern Medical Center at Dallas, 5323 Harry Hines Blvd., Dallas, Texas 75235, USA

Background: The mitogen-activated protein (MAP) kinase, ERK2, is a tightly regulated enzyme in the ubiquitous Ras-activated protein kinase cascade. ERK2 is activated by phosphorylation at two sites, Y185 and T183, that lie in the phosphorylation lip at the mouth of the catalytic site. To ascertain the role of these two residues in securing the low-activity conformation of the enzymes we have carried out crystallographic analyses and assays of phosphorylation-site mutants of ERK2.

Results: The crystal structures of four mutants, T183E (threonine at residue 183 is replaced by glutamate), Y185E, Y185F and the double mutant T183E/Y185E, were determined. When T183 is replaced by glutamate, few conformational changes are observed. By contrast, when Y185 is replaced by glutamate, 19 residues become disordered, including the entire phosphorylation lip and an adjacent loop. The conservative substitution of phenylalanine for Y185 also induces relatively large conformational changes. A binding site for phosphotyrosine in the active enzyme is putatively identified on the basis of the high-resolution refinement of the structure of wild-type ERK2.

Conclusions: The remarkable disorder observed throughout the phosphorylation lip when Y185 is mutated shows that the stability of the phosphorylation lip is rather low. Therefore, only modest amounts of binding energy will be required to dislodge the lip for phosphorylation, and it is likely that these residues will be involved in conformational changes associated both with binding to kinases and phosphatases and with activation. Furthermore, the low-activity structure is specifically dependent on Y185, whereas there is no such dependency on T183. Both residues, however, participate in forming the active enzyme, contributing to its tight control.

Structure 15 March 1995, **3**:299–307
Key words: crystallography, MAP kinase ERK2, MEK, phosphorylation sites

Introduction

The mitogen-activated protein (MAP) kinase, ERK2 (extracellular signal-regulated kinase 2), is an important transducer of information from the cell surface to intracellular targets [1–5]. The activity of ERK2 is tightly regulated. Dual phosphorylation events, one on residue Y185 and one on T183 are required for ERK2 activation [2,6,7]. Both of the phosphorylation reactions are catalyzed [8] by the same kinase, MEK (MAP/ERK kinase) [9,10], although the phosphorylation of Y185 is preferred kinetically [11]. Inactivation of ERK2 is achieved independently through the action of serine/threonine phosphatases, tyrosine phosphatases [2,12], or dual-specificity phosphatases [13,14], demonstrating that both covalently bound phosphates are required to maintain high activity. Thus, while a single type of enzyme (MEK) activates the MAP kinases, multiple pathways may lead to their inactivation.

We have previously determined the structure of unphosphorylated, low-activity ERK2 [15]. The phosphorylation sites Y185 and T183 are in the phosphorylation lip (between subdomains VII and VIII), a 15-residue surface loop near the mouth of the active site (Fig. 1). In unphosphorylated ERK2, Y185 is found largely buried, whereas T183 is on the surface. The sequence of this lip is hypervariable among the protein kinases [16]. Likewise, the structure of this region varies greatly among the protein kinases for which structures are available [17]. Based on the following observations, the phosphorylation lip probably adopts a considerably different conformation in the active form of the enzyme [15]. First, in the low-activity structure, the lip blocks the substrate-binding site. Second, the residues that form the phosphate-binding site for T197 in cyclic AMP dependent protein kinase (cAPK) are conserved in ERK2 [15], yet in unphosphorylated ERK2, neither of the phosphorylation site residues is close enough to interact with this site. Interaction of a phospho-amino acid with this site may be important in promoting the closed-domain configuration observed in cAPK [18]. Finally, as Y185 is buried, the phosphorylation lip must assume a different conformation when bound to MEK.

Several ERK2 mutants have previously been synthesized and characterized to help in understanding the roles of the individual phosphorylation sites in the activation of the enzyme [10]. The published results most relevant to the present study are that the mutant T183E can be phosphorylated and partially activated by MEK, whereas the Y185F mutant can be phosphorylated by MEK but is not active. Here we describe the enzymatic properties of

*Corresponding author.

 ISSN 0969-2126

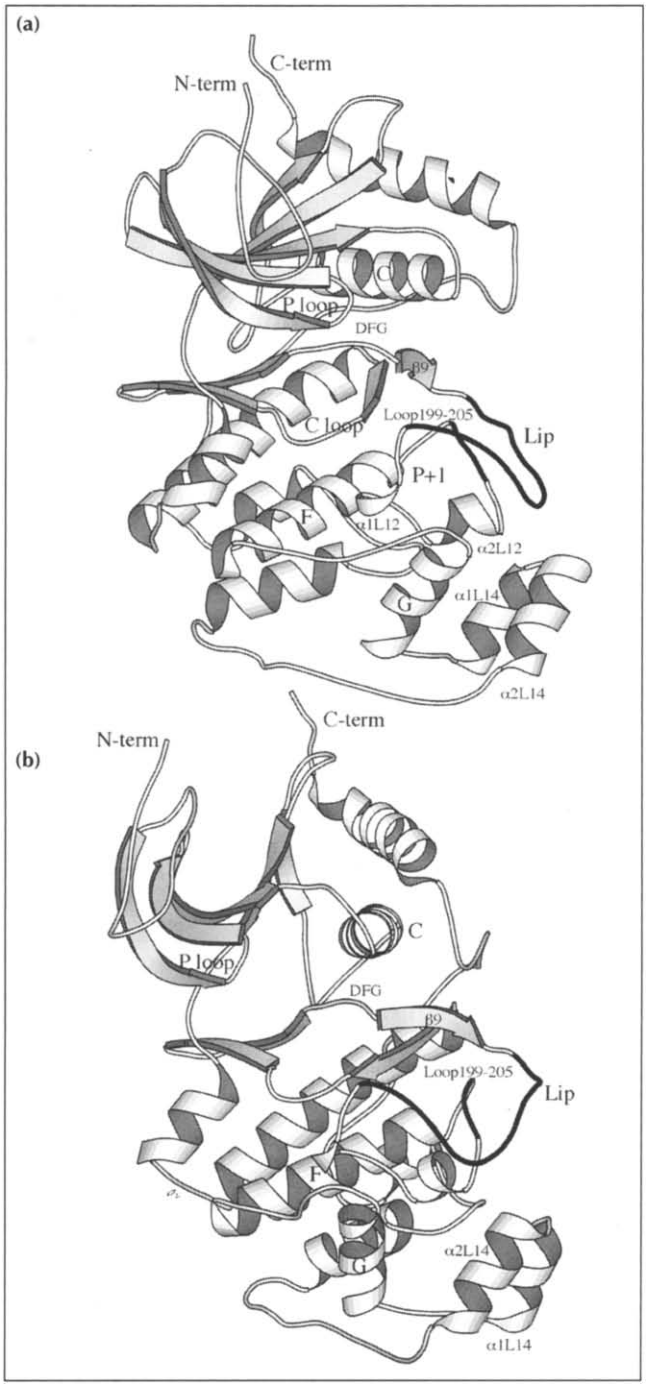

Fig. 1. Ribbon diagram of ERK2 drawn by Molscript [34]. **(a)** Standard kinase view; **(b)** view 45° rotation about the vertical axis. The disordered regions in the mutant Y185E or the double mutant T183E/Y185E are shown in black; the lip and loop199–205 are defined by residues 173–197 and 202–203, respectively. The 'C loop' is the catalytic loop, subdomain VI. The 'P loop' is the phosphate-binding site for ATP. The nomenclature used is based on the secondary-structure elements assigned in [18]. Intervening sequences, or linkers, are labeled L based on the terminology in [17], starting at L_0, at the N-terminal extension from the core kinase domain. A few short helices that are not assigned in [18], are labelled here as linkers. α2L12 refers to the second helix in L12, etc.

the additional mutant enzymes Y185E, T183E/Y185E, and T183E/Y185G. The data show that glutamate can

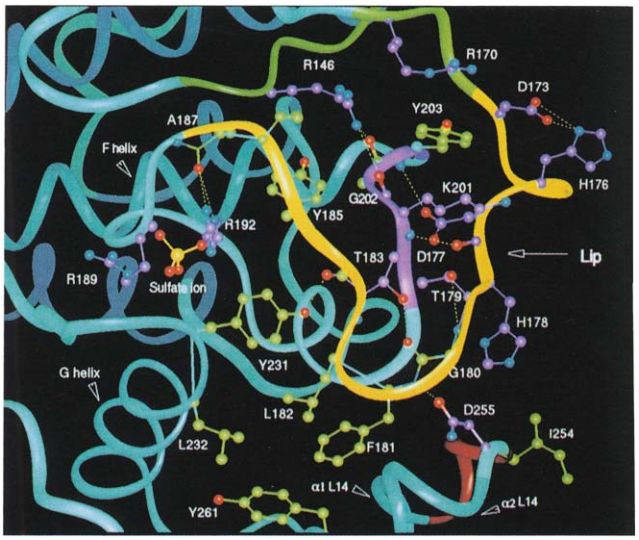

Fig. 2. The phosphorylation lip region drawn in INSIGHT. Regions that are disordered in the mutants are colored as follows: the phosphorylation lip is yellow, residues S200–Y203 in loop199–205 are purple, and E251–I254 in L14 are brown. β-strands are shown in green and α-helices are shown in dark blue with other regions in lighter blue. The carbon atoms of hydrophobic residues are colored green and those of polar or charged residues are colored purple. A sulfate ion is shown as red and yellow spheres. Hydrogen bonds are shown as dashed lines.

partially substitute for phosphothreonine to form the active enzyme once Y185 is phosphorylated, but glutamate mimics phosphotyrosine only poorly in the active structure. Furthermore, glycine does not substitute for Y185, showing that phosphotyrosine is required to form the active enzyme.

To explore how Y185 of the wild-type enzyme might become available for phosphorylation by MEK, and to understand the roles of the phosphorylation-site residues in the activation of the molecule, we have determined the structures of four of these ERK2 mutants in the unphosphorylated state. The structures of these mutants do not give us a detailed picture of the active conformation of the molecule. Instead, the crystallographic analysis shows that the stability of the phosphorylation lip is low, and suggests which residues may be involved in conformational changes associated with activation. In addition, on the basis of the refinement of the wild-type enzyme structure, an anchoring site for phosphotyrosine on the surface of the active enzyme is proposed. Together, the activity and crystallographic data reveal essential functions for Y185 in both the inactive and active states of the protein kinase.

Results

Anatomy of the phosphorylation lip of unphosphorylated wild-type ERK2

The ERK2 phosphorylation sites, T183 and Y185, are in the lip (Figs 1,2,3) that links subdomains VII and VIII as defined by Hanks *et al.* [16]. The lip is part of L12, the linker between the secondary-structure elements β9 and

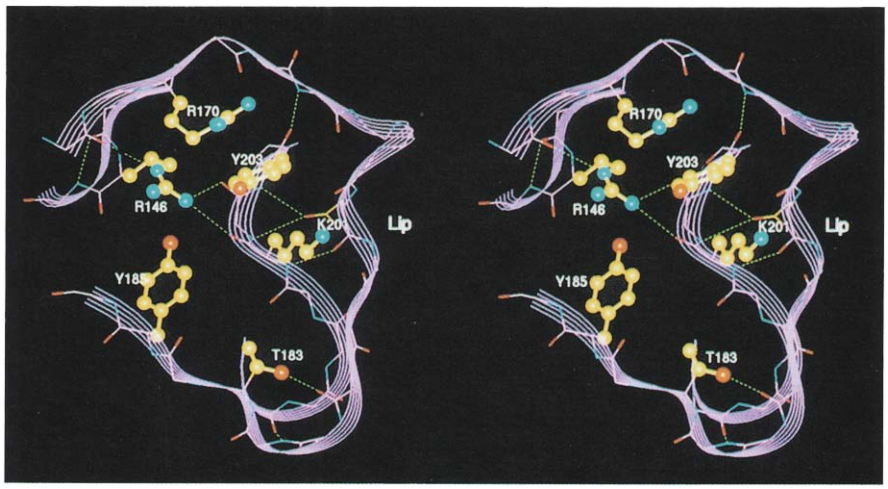

Fig. 3. Stereodiagram emphasizing the interaction between the lip and loop199–205 region.

F-helix (nomenclature defined in [17], and in Fig. 1 legend). In ERK2, the lip consists of 15 residues, D173–A187 (DPDHDHTGFLTEYVA) and is near the mouth of the active site. The side chain of T183 is found on the surface of the molecule, whereas the side chain of Y185 is largely buried.

Much of the structure of the lip is lost in the mutants described below. Yet, the structure of the lip in wild-type ERK2 is well defined (see electron density in Fig. 4a). In wild-type ERK2, the B-factors for the main-chain atoms in the lip range from 27 Å^2–45 Å^2, slightly higher than the average B-factor for the remainder of the C-terminal domain, which is 22 Å^2. The residues that flank the phosphorylation sites, L182, E184, and V186, have B-factors of over 50 Å^2, as is obvious from the weak electron density on these residues (Fig. 4a).

The lip makes an unusual interaction with a neighboring loop, which comprises residues N199–K205 (labeled loop199–205 in Fig. 1a,b). The lip and loop199–205 form a semi-compact structure (Fig. 3). A hydrophobic stacking

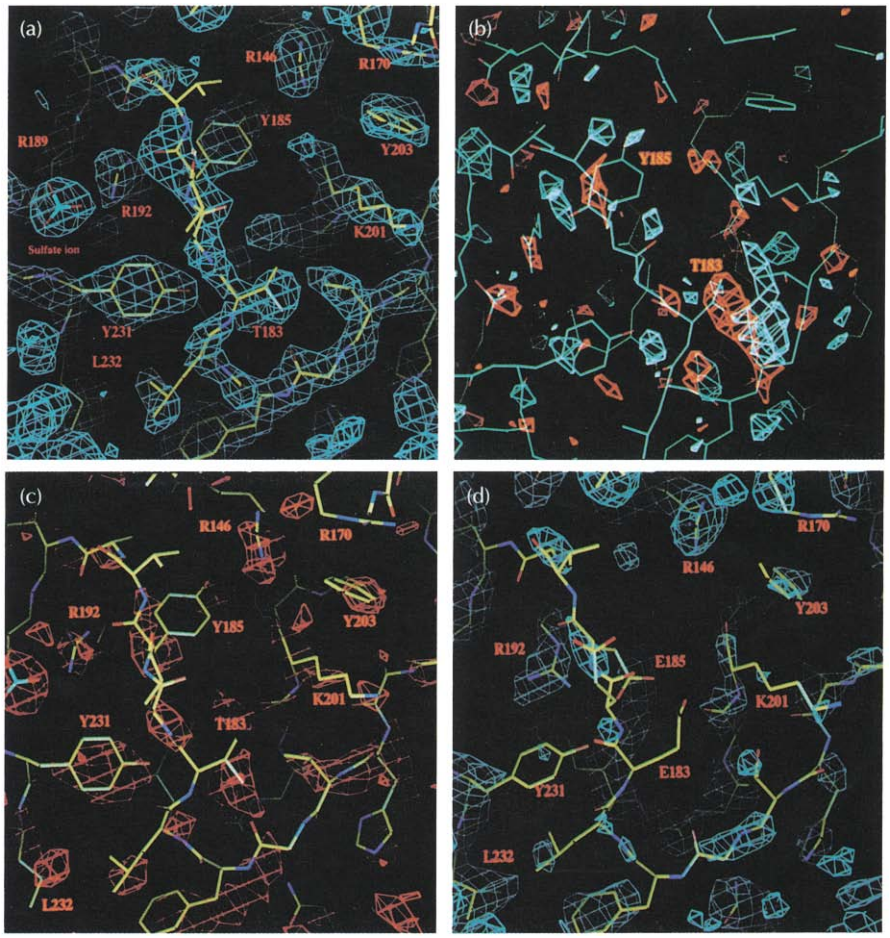

Fig. 4. Electron-density maps drawn in O [29]. **(a)** The 2Fo–Fc map of the wild-type ERK2 around the lip calculated with data from 6–2.3 Å contoured at 1.25σ. **(b)** T183E difference map computed with ($|Fo_{mutant}|-|Fo_{wild\text{-}type}|$) coefficients from 20–2.3 Å and native model-derived phases (a) contoured at 2.5σ. Positive density is shown in blue. Negative density is shown in brown. **(c)** The ($|Fo_{(mutant)}|-|Fo_{(wild\text{-}type)}|$ T183E/Y185E contoured at −2.5σ. **(d)** The 2Fo–Fc map of T183E/Y185E computed with refined phases and contoured at 1.25σ.

interaction clusters R170, K201 and Y203 (Figs 2,3) at the center, and the lip is wrapped around the outside, reminiscent of an Ω-loop. There are two connecting hydrogen bonds (D177O–K201N and D177Oδ1–Y203N). In ERK2, the guanidinium group of R146 also forms two hydrogen bonds to the backbone of loop199–205. Interestingly, the residues that form the hydrophobic stack are also conserved in several other kinases, including cAPK. However, in cAPK the interactions at this site are quite different: Y215(203) forms an electrostatic interaction with R165(146) (similar to Y185 in ERK2, see below) and K213(201) faces the solvent. With R146 in close proximity, three positively charged residues are clustered. Two of these, R146 and R170, contribute to the conserved phosphate-binding site identified in cAPK. The sequences of the lip and loop199–205 are linked by the P+1 specificity pocket (residues T188–R192) and a six-residue α-helix (A193–L198) (labeled α2L12, in Fig. 1a).

The lip also makes contacts with the remainder of the structure. Y185 is the focus of a hydrophobic patch where one face of the phenyl ring makes extensive contacts with R192 (in the P+1 specificity pocket) and I196 in α2L12 (Fig. 3). The opposite face of the phenyl ring makes loose contacts with A187 and G202, while Y185Oη is close to R146Nη1 (3.5 Å). Another hydrophobic patch centers around F181 and L182. These residues lie in a surface depression consisting of L198 in α2L12, L232 in the G-helix, and A258 and Y261 in α2L14 α-helix that is part of a large insertion in ERK2 relative to cAPK (Fig. 3). Hydrogen bonds and ion pairs are also present within the lip and connect the lip to the surrounding structure. Internal to the lip, hydrogen bonds link T179Oγ and G180N, T183Oγ and G180O, and D173Oδ1,2 and H176Nδ1. Two bonds link the lip to loop199–205, as described above. Three other hydrogen bonds link A187O and R192Nη1 (in the P+1 specificity pocket), F181N and N255Oδ1 (in the L14 insertion), and E184O and Y231Oη (at the N terminus of the G-helix). H178Nδ1 forms a hydrogen bond with T157O of a neighboring molecule in the crystal lattice. In total, 11 hydrogen bonds stabilize the low-activity conformation of the lip.

Table 1. Activity of wild-type and mutant ERK2 before and after phosphorylation with MEK kinase.

Molecule	Activity (nmol min^{-1} mg^{-1}) –	Activity (nmol min^{-1} mg^{-1}) +
Wild-type	1.4	1360
T183E	1.2	94
Y185E	0.7	5.2
Y185F	0.7	6.2
T183E/Y185E	0.9	–
T183E/Y185G	0.7	–

Table 2. Statistics of data collection, scaling and refinement.

Crystal	Native	T183E	Y185E	Y185F	Y185E/T183E
Data					
Resolution (Å)	2.3	2.3	2.7	3.5	2.5
Reflections measured	62796	37906	27790	20251	22412
Unique reflections	17755	15258	10203	4408	12035
Completeness (%)	99	85	92	90	85
R_{sym}[a] (%)	5.1	2.5	4.43	4.8	5.18
Refinement					
Resolutions (Å)	6–2.3	6–2.3	6–2.7	6–3.5	6–2.5
Reflections (F/σ>2)	15202	13895	8608	3980	11030
Scale factors	1	0.718	1.831	2.227	0.204
Scale B-factors (Å^2)	0	0.9	2.5	0	−11.8
Water molecules	80	0	0	0	0
R-factor[b]	16.4%	19.0%	15.8%	15.2%	17.0%
Free R-factor[c] (%)	21.5	23.2	23.0	18.8	22.5
Geometry deviations:					
Rms bonds (Å)	0.010	0.011	0.010	0.010	0.090
Rms angles (°)	1.54	1.61	1.62	1.62	1.63
Rms B-factor[d] (Å^2)	2.0	1.8	2.5	2.0	2.5
Rms Cα shift[e] (Å)		0.38	0.21	0.26	0.36

[a] $R_{sym} = \Sigma|Ii - \langle I \rangle| / \Sigma Ii$, where Ii is the intensity of an individual measurement and $\langle I \rangle$ is the mean value of its equivalent reflections. [b] R-factor = $\Sigma||Fobs| - |Fcalc|| / \Sigma|Fobs|$, where |Fobs| and |Fcalc| are the observed and calculated structure-factor amplitudes respectively. [c] Free R-factor was calculated using a subset of data (10%) which was excluded from refinement until the last round. [d] Rms B-factor was calculated for the main-chain atoms within each residue. [e] Rms Cα shift of the mutants relative to the wild-type was calculated without the disordered residues in the wild-type and the disordered lip.

Enzymatic properties of mutant ERK2 molecules

ERK2 mutants with altered phosphorylation sites were synthesized to ascertain the role of these residues in activation. Single-residue mutations in the phosphorylation sites of ERK2 have little effect on the basal activity, although they do interfere with the activation of ERK2 by phosphorylation. In a previously published study [10], the tyrosine phosphorylation site was removed from ERK2 by replacing Y185 by phenylalanine. This mutant enzyme could no longer be activated above the basal level. Also, a glutamate was substituted at position 183 to mimic the effect of phosphothreonine. T183E was demonstrated to be phosphorylated on Y185 and activated to 10% of the wild-type levels (Table 1). Additional mutants were synthesized to ascertain whether a constitutively active ERK2 could be synthesized by introducing glutamate residues at the phosphorylation sites in Y185E and the double mutant T183E/Y185E. A second double mutant T183E/Y185G was made to determine whether Y185 has any role other than to sterically inhibit the enzyme in the low-activity structure, as suggested previously [15]. None of these mutants has enhanced basal activity. Y185E, which retains a phosphorylation site, can be phosphorylated by MEK (~0.4 mol mol^{-1}) and weakly activated (Table 2). The double mutants have only basal levels of activity.

Taken together, these data show that glutamate at position 183 can partially substitute for phosphothreonine in the active structure, when Y185 is phosphorylated. However, glutamate at position 185 can substitute only

poorly for phosphotyrosine to form the active structure when T183 is phosphorylated. Furthermore, because the double mutant T183E/Y185G has only basal activity, Y185 may have a role in forming the active structure.

Crystallographic analysis of the mutant enzymes

Crystallization conditions similar to those used for the native enzyme were effective in producing crystals of the mutants T183E, Y185F, Y185E, and the double mutant T183E/Y185E. Data were collected on the mutant enzymes to a resolution comparable, in most cases, to that of the native enzyme, 2.3 Å. The only exception is Y185F for which only small crystals that diffracted to 3.5 Å could be obtained. The structures were refined as described in the Materials and methods. In the wild-type enzyme, the lip and surrounding structure are well defined in the electron-density map (Fig. 4a), with the exception of residues L182, E184 and V186 as noted above.

The mutant T183E

The differences between the mutant and wild-type enzyme are observed in the difference map (Fig. 4b) computed as described in the legend to Fig. 4. In the final refined model, few structural changes are observed. Disorder is introduced in residues E183 and A187 by the mutation. As noted above, residues that flank the phosphorylation sites are disordered in the wild-type enzyme; thus, in this mutant the electron density is weak from E183–A187 (Table 3). Y185, however, remains fixed. Hydrogen bonds between T183Oγ and G180N and between A187O and R192Nη1 are lost, apparently as a consequence of the disorder introduced. The overall root mean square (rms) shifts of Cα atoms, calculated for residues that do not become disordered, are ~0.25 Å (Table 2), which is no larger than the coordinate error.

Thus, it is possible to conclude that T183 makes a small contribution to the stability of the low-activity conformation of ERK2, and introduction of a charge at position 183 may disrupt this structure slightly.

The mutants Y185E and T183E/Y185E

The structures of two mutant enzymes containing a glutamate at position 185 were determined, Y185E and the double mutant T183E/Y185E containing a glutamate at both positions 183 and 185. The difference map for both of these mutants (Fig. 4c) shows negative density throughout the entire lip (residues D173–A187) and in loop199–205 between residues S200 and Y203 (Table 3; Fig. 4c). In the double mutant, the difference map of which is shown in Fig. 4c, the negative density is more pronounced than in the single mutant, and includes N251–I254 in α1L14 and E58–C63 near the N terminus of helix C. The disorder is also apparent from the refined electron-density map (Fig. 4d). The density is broken and weak around the lip, whereas neighboring residues such as R146 and D147 (Fig. 4d) are well defined. The residues that become disordered are summarized in Table 3. In mutant Y185E, 19 residues are disordered in the lip and loop199–205. The carboxylate of E185 is weakly visible in the Y185E mutant but not in the double mutant T183E/Y185E. The side chain of F181, which resides in one of the hydrophobic patches, is weakly observed, despite disorder in its main chain. However, K201, Y203 and the side chain of R170 in the hydrophobic stack are disordered, and their interactions with the lip are lost. Also, all of the hydrogen bonds internal to the lip, and between the lip and the rest of the molecule, are lost in the mutants containing a glutamate at position 185. The interactions that are lost are those between D177O and K202N, D177Oδ1 and Y203N, F181N and N255Oδ1, E184O and Y231Oη, A187O and R192Nη1, and between R146Nε1 and K201O and G202O. The residues that are linked by a hydrogen bond to the lip in the native structure are shifted or disordered in the mutant enzymes. For example, the guanidinium groups of R146 and R192 are displaced by ~1.0 Å, but remain ordered in both Y185E and T183E/Y185E. In contrast, the side chain of Y231 becomes disordered. The lattice contact formed by H178 in the lip is lost.

Table 3. Disorder in ERK2 mutants.

Mutant	Location	Disordered residues
Wild-type	main chain	V186
	side chain	L182, E184, V186
T183E	main chain	E183, V186, A187
	side chain	L182, E184, E183, V186, A187
Y185E	main chain	D173–A187, S200–Y203
	side chain	D173–G180, L182–A187, S202–Y203, Y231
T183E/ Y185E	main chain	D173–A187, S202–Y203, E58–C53, N251–I254
	side chain	D173–G180, L182–A187, S202–Y203, Y231, E58–C53, N251–I254
Y185F	main chain	D173–A187, E58–C53
	side chain	D173–G180, L182–E184, V186–A187, E58–C53

Named residues have B-factors in excess of 50 Å^2 for T183E, Y185E and T183/Y185E.

Although the structural basis for the low stability is uncertain, it may be due to the unusual cluster of three positively charged amino acids R146, R170, and K201. As noted above, these cluster at the core of the interaction between the lip and loop199–205 (Fig. 3), and although the residues involved are conserved between ERK2 and cAPK, the nature of the interaction is completely different in the two molecules.

The B-factors of the main-chain atoms of native ERK2 are shown in Fig. 5a. The B-factors in the wild-type enzyme are elevated at the termini of the molecule and in a few other loops (Fig. 5a). The shift in B-factors in the mutants is shown in Fig. 5b. The B-factors in T183E are elevated in the lip (173–188), and loop199–205, as discussed below. The B-factors in the double mutant are elevated in two other regions, centered around N251–I254 and E58–C63. The data set for T183/Y185

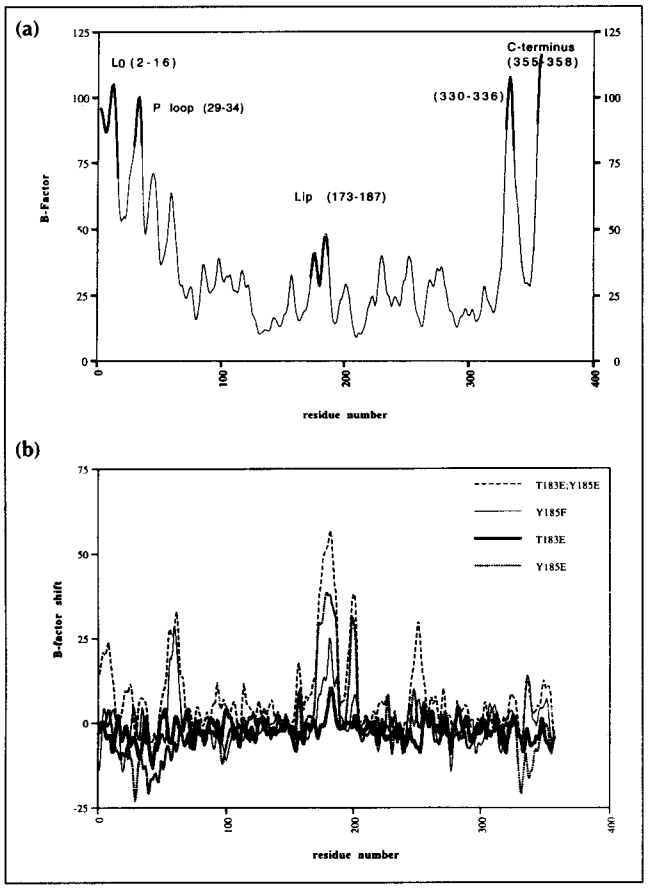

Fig. 5. **(a)** Plot of B-factors (temperature factors in Å) of the main-chain atoms as a function of sequence of the wild-type ERK2. The average B-factor of ordered main-chain atoms is 29.8 $Å^2$. The average B-factor of the main-chain atoms from residues 63–327 is 24.5 $Å^2$, from residues 17–62 and from residues 328–358 is 52.9 $Å^2$. **(b)** Plot of shifts in B-factor of main-chain atoms in ERK2 mutants relative to wild-type. In T183E/Y185E, the B-factor shifts for the indicated residues were as follows: residues 58–63 over 35 $Å^2$, 173–187 over 45 $Å^2$, 197–203 over 30 $Å^2$, and 248–254 over 25 $Å^2$. In T183E, the lip region has B-factor shifts over 30 $Å^2$, and residues 198–203 over 20 $Å^2$.

gives a relatively large scaling B-factor (Table 2), suggesting that there is some general disorder in the crystal of this double mutant. However, the changes in B-factor local to the lip are independent of the scaling method.

Mutant Y185F

Like Y185E, Y185F has negative density on the phosphorylation lip in the difference map (data not shown). Although, the resolution of the Y185F data is limited, it is possible to carry out a partial refinement using Powell minimization in X-PLOR. The refined model from this analysis reveals disorder throughout the phosphorylation lip. However, the level of disorder is less than in the other Y185 mutants, with an average shift in the B-factor of 15 $Å^2$. The disorder does not extend to loop199–205. F185 occupies a position similar to Y185 in the wild-type enzyme, but is found shifted away from R146. This displacement could be due to loss of the favorable electrostatic interaction between Y185Oη and R146Nη1. From the disorder in this mutant we can conclude that the loss of a single atom, the hydroxyl oxygen of Y185, disrupts the structure of the lip.

B-factor shifts

When the shifts in B-factors for all of the mutants are compared (Fig. 5b), it is apparent that the B-factor shifts for each mutant occur in the same parts of the molecule. Thus, whereas Y185E exhibits the largest changes for a point mutation, the other three mutants cause correlated changes. The correlated nature of the B-factor shifts in the different mutants shows that the flexibility is a property of the molecule and not due to the specific amino acid replacement.

Interestingly, the T183E/Y185E double mutant shows disorder in two sequences distant from the lip. One region is unique to the ERK family (N251–I254) and the other lies near the N terminus of helix C, where the structure of ERK2 diverges significantly from that of cAPK and cyclin dependent kinase 2 (CDK2). Therefore, it is expected that these regions are important for either substrate specificity or regulation of ERK2. Region N251–I254 (in α1L14) interacts with the lip, but helix C does not contact the lip, so that the origin of the disorder in E58–C63 is unclear. It may be that this disorder and the slight elevation of the B-factors in the double mutant is a consequence of lattice contact losses, as I254 is involved in a lattice contact. The negative B-factor shifts in Y185E near the N and C termini are probably insignificant, and due to the large B-factors in the wild-type enzyme in these areas of the structure (Fig. 5a).

Putative binding site for both phosphotyrosine and phosphothreonine

ERK2 may have two phosphate-binding sites to accommodate the two phosphorylated residues in the active enzyme. One likely binding site, which appears to be conserved among many serine/threonine-specific kinases, consists of residues R146 and R170 (see above) and R65 in helix C in ERK2 [15,17,19]. This phosphate-binding site is also conserved in the kinase ERK3. ERK3 has a threonine at position 183 but a glycine at position 185. Therefore, T183–PO_4 is likely to bind to the conserved site. A significant rearrangement of the lip is required to obtain this interaction, because in the low-activity structure T183 is ~9 Å from R146. This binding interaction may promote domain rotation in ERK2 to create a closed catalytic site similar to that found in cAPK [15]. For the conserved R146 to bind to a phosphate ion, it must lose its interactions with the backbone of loop199–205. It is interesting that these interactions are indeed lost in two of the mutants described above.

ERK2 has a second cluster of positively charged residues near the phosphorylation lip. This cluster consists of R189 and R192, and is not conserved in other kinases. Further refinement of the wild-type crystal structure carried out in this study, revealed a sulfate ion, present in the crystallization buffer, in contact with R189 and R192 (Figs 2,3). These residues are close to Y185, in the P+1

specificity pocket identified in cAPK [20]. Although the primary function of Y185 appears to be in securing the low-activity conformation, Y185–PO_4 may play a role in the active conformation. Biochemical evidence for this suggestion can be derived from the low activity of the double mutant T183E/Y185G: if Y185 were acting solely to secure the inactive conformation by binding in its inhibitory site, then removing its side chain might have been expected to create a constitutively active enzyme in T183E/Y185G. However, this is not the case. Therefore, these two arginines may serve as the second phosphate-binding site in the active conformation of ERK2, and bind to Y185–PO_4.

Discussion

The phosphoregulation of protein kinases is highly unusual. Many of the phosphorylation sites reside in a single loop at the mouth of the catalytic site. In ERK2, Y185 phosphorylation is kinetically favored, even though the residue is buried within the structure. Both of the phosphorylation-site residues are out of alignment with potential phosphate-binding ligands on the surface of the enzyme. Consequently, several mechanistic questions arise: first, how do the phosphorylation-site residues become available for phosphorylation; second, what are the roles of the individual phosphorylation sites in the activation mechanism; and finally, how much of the structure is involved in the conformational changes associated with activation? Furthermore, several general questions arise concerning the way in which different mechanisms of regulation are accommodated in this region and by which the active sites of associated kinases and phosphatases co-evolve. The remarkable degree of disorder observed when Y185 is mutated lends insights into many of these questions.

The disorder observed in the mutant ERK2 enzymes studied here, shows that the stability of the lip region is rather low. Changes such as point mutations, or introduction of buried charges, do not ordinarily lead to significant loss of structure [21]. As the stability is low, it is expected that only modest amounts of binding energy, supplied by the activating enzyme, are required to dislodge Y185 for phosphorylation. The preferential phosphorylation of Y185 may simply result from a more favorable interaction when Y185 is bound in the active site of MEK. The disorder throughout the lip region also suggests that the entire lip changes conformation when bound to the activating enzyme. Interestingly, a modeling study of known tryptic cleavage sites in proteins of known structure shows that at least 12 residues must change conformation for the cleavage site to fit into the trypsin active site [22]. Modeling shows that a similar number of conformational changes are required to allow binding of the lip of ERK2 to the active site of MEK.

The disorder observed in Y185 mutants but not in T183 mutants provides information about the roles of these residues in activation. Y185 has a primary function in securing the inactive conformation of the enzyme: mutation of Y185 to a glutamate or phenylalanine causes extensive disorder. Because the conformational changes and disorder associated with the replacement of T183 are much less pronounced than those in Y185 mutants, it seems that T183 is less important in the low-activity structure. On the other hand, both residues once phosphorylated may participate in the active conformation, and two putative sites for binding of phosphothreonine 183 and phosphotyrosine 185 have been identified.

Local refolding appears to be required to bring either of the phosphorylation-site residues into alignment with the conserved phosphate binding site observed in cAPK [18], or with the putative phosphate-binding site described above. It is interesting in this regard that introducing a negative charge at position 185 induces extensive disorder, suggesting that the low-activity conformation is inconsistent with a charge at this position. Refolding is apparently also required in CDK2 to bring T161 into alignment with the conserved phosphate-binding site [17]. It may be that refolding is involved in the activation of other kinases as well. This mechanism, involving refolding of a surface loop, is distinct from that observed in isocitrate dehydrogenase, which is also phosphorylated near the catalytic site [23]. However, refolding is reminiscent of the order–disorder transition observed in other active sites, for example, that of triose phosphate isomerase [24].

Biological implications

Many protein kinases are regulated by phosphorylation that takes place within a short region of their polypeptide sequence, known as the lip, which is near the active site. In any one molecule, the lip must assume at least four different conformations — the inactive and active structures, and the structures as bound to their activating and deactivating enzymes. Although no structural data are yet available for unphosphorylated and phosphorylated forms of the same enzyme, comparison of the available kinase structural data suggests that the lip is likely to be folded differently in the active and inactive structures. Extracellular signal-regulated kinase 2 (ERK2) is a very tightly regulated kinase in the ras-activated protein kinase cascade and has two phosphorylation sites within the phosphorylation lip, a tyrosine and a threonine. Phosphorylation by the MAP/ERK kinase (MEK), occurs first on the tyrosine residue that is buried in the unphosphorylated enzyme, but phosphorylation of the threonine residue is also required to produce the active enzyme.

We mutated the tyrosine and threonine phosphorylation-site residues to glutamate and phenylalanine to study the role of each site in activation. None of the mutants produced a constitutively active enzyme, in the absence of phosphorylation at the

second site. This is consistent with the fact that no oncogene derived from the ERK2 gene has been observed. The crystallographic analysis described here reveals that the entire lip is disordered when certain point mutations are introduced within the regulatory sequence. This shows that the stability of the 19-residue lip is low, and provides further evidence for the theory that the lip may be refolded in the active structure. This low stability may be an important factor in the binding of the lip region of ERK2 to kinases and phosphatases, and helps to explain the fact that the phosphorylation of the buried tyrosine is kinetially favored. Regulatory sequences that occur in the termini of other molecules are known to undergo order/disorder transitions [25]. Surprisingly, however, the protein kinases the flexible regulatory sequence is internal to the polypeptide chain. The close proximity of the phosphorylation lip to the active site may facilitate the tight regulation observed in the MAP kinases — regulation that is acheived without additional regulatory sequences or subunits.

Materials and methods

Expression, assay, and mutagenesis

ERK2 and mutants were expressed in *Escherichia coli* using the expression vector NpT7-5 with an incorporated hexahistidine tag to aid purification. Point mutations were introduced into ERK2 as described in [10]. Assay of basal kinase activity towards myelin basic protein (MBP) was carried out using 0.01 μg ml^{-1} ERK2, 0.3 mg ml^{-1} MBP, and 100 μM ATP ([γ^{32}P]ATP, 1–10 cpmf mol^{-1}) in 5 mM HEPES buffer pH 8.0, 10 mM β-glycerol phosphate, and 0.2 mg ml^{-1} bovine serum albumin at 30°C for 1 h. ERK2 was activated by incubation with MEK1 (50 μg ml^{-1}). The MEK1, in turn, was activated with the catalytic domain of MEK kinase (Xu, S.C. *et al.*, unpublished data). The specific activity of activated ERK2 was determined as above, at an ERK2 concentration of 0.2 mg ml^{-1}.

Crystallization, data collection, and scaling

Recombinant ERK2 mutant molecules were expressed, purified and crystallized as described in [26]. All of the mutants that crystallized did so in the same space group as the wild-type enzyme, $P2_1$, with similar cell constants. Data for Y185F, T183E and Y185E were recorded using Xuong-Hamlin area detectors in 0.10 frames and X-rays generated on an Rigaku RU200 rotating anode source operated at 50 kV, 100mA. Data for the double mutant T183E/Y185E were collected using R-axis II imaging plates in 2° oscillations. Data sets for the mutant enzymes were scaled to the wild-type data set so that the individual atomic B-factors were on a common scale. Scaling was carried out in PROTEIN [27]. The B-factors were obtained from refinement using the mutant data that were scaled individually with the wild-type in PROTEIN [27]. Data statistics and scale factors are summarized in Table 2.

Refinement

The model reported in [15] was further refined at 2.3 Å (Table 2). The present model of the wild-type enzyme includes 80 water molecules and one sulfate ion. The wild-type model was used as a starting point for refinement of the mutants. The water molecules were omitted. Powell minimization was carried out in X-PLOR [28] for all of the mutants. T183E, Y185E and T183E/Y185E were further refined using molecular dynamics simulation with an initial temperature of 1000 K. Individual atomic B-factors were refined using restraints of 1.5σ for main-chain atoms and 2.0σ for side-chain atoms. After each cycle, the model was fitted to a 2|Fobs|−|Fcalc| map calculated with refined phases in programs O [29] or FRODO [30]. Only one cycle of Powell minimization and temperature-factor refinement was carried out for Y185F because of the lack of data. In the final model of the native enzyme, residues 2–16, 29–34, 330–336 and 355–358 have weak density and are disordered. All of the peptide torsion angles of the native and mutant models fall within the most favored regions or additional allowed regions of the Ramachandran (ϕ,ψ) diagram as defined in [31], except for R146. This residue has been checked by modeling, and appears to be correct. Stereochemical parameters measured in PROCHECK [32], were found to have better than 'ideal' values [33]. These stereochemical parameters include: percentage of residues in the most favorable regions of the Ramachandran diagram, number of close contacts, hydrogen bond energy, and the standard deviations of various torsion angles, ω, z, χ1 and χ2.

The coordinates will be deposited in the Brookhaven Protein Data Bank.

Acknowledgements: This research was supported by the American Heart Association and the Welch Foundation (#I1128) and in later stages by the NIH (DK46993).

References

1. Boulton, T.G., *et al.*, & Cobb, M.H. (1990). An insulin-stimulated protein kinase similar to yeast kinases involved in cell cycle control. *Science* **249**, 64–67.
2. Anderson, N.G., Maller, J.L., Tonks, N.K. & Sturgill, T.W. (1990). Requirement for integration of signals from two distinct phosphorylation pathways for activation of MAP kinase. *Nature* **343**, 651–653.
3. Schaap, D., van der Wal, J., Howes, L.R., Marshall, C.J. & van Blitterswijk, W.J. (1993). A dominant-negative mutant of Raf blocks mitogen-activated protein kinase activation by growth factors and oncogenic p21ras. *J. Biol. Chem.* **268**, 20232–20236.
4. Lange-Carter, C.A., Pleiman, C.M., Gardner, A.M., Blumer, K.J. & Johnson, G.L. (1993). A divergence in the MAP kinase regulatory network defined by MEK kinase and Raf. *Science* **260**, 315–319.
5. Robbins, D.J., Zhen, E., Cheng, M., Xu, S., Ebert, D. & Cobb, M.H. (1994). MAP kinases ERK1 and ERK2: pleiotropic enzymes in a ubiquitous signaling network. *Adv. Cancer Res.* **63**, 93–116.
6. Ahn, N.G., Seger, R., Bratlien, R.L., Diltz, C.D., Tonks, N.K. & Krebs, E.G. (1991). Multiple components in an epidermal growth factor-stimulated protein kinase cascade. *J. Biol. Chem.* **266**, 4220–4227.
7. Payne, D.M., *et al.*, & Hunt, D.F. (1991). Identification of the regulatory phosphorylation sites in pp42/mitogen-activated protein kinase (MAP kinase). *EMBO J.* **10**, 885–892.
8. Her, J.-H., *et al.*, & Weber, M.J. (1993). Dual phosphorylation and autophosphorylation in mitogen-activated protein (MAP) kinase activation. *Biochem. J.* **296**, 25–31.
9. Seger, R., *et al.*, & Ericsson, L. (1992). Human T-cell mitogen-activated protein kinase kinases are related to yeast signal transduction kinases. *J. Biol. Chem.* **267**, 25628–25631.
10. Robbins, D.J., *et al.*, & Cobb, M.H. (1993). Regulation and properties of extracellular signal-regulated protein kinases 1 and 2 *in vitro*. *J. Biol. Chem.* **268**, 5097–5106.
11. Haystead, T.A., Dent, P., Wu, J., Haystead, C.M.M. & Sturgill, T.W. (1992). Ordered phosphorylation of p42mapk by MAP kinase kinase. *FEBS Lett.* **306**, 17–22.
12. Boulton, T.G. & Cobb, M.H. (1991). Identification of multiple extracellular signal-regulated kinases (ERKs) with antipeptide antibodies. *Cell Reg.* **2**, 357–371.
13. Zheng, C.-F. & Guan, K.-L. (1993). Dephosphorylation and inactivation of the mitogen-activated protein kinase by a mitogen-induced Thr/Tyr protein phosphatase. *J. Biol. Chem.* **268**, 16116–16119.

14. Sun, H., Charles, C.H., Lau, L.F. & Tonks, N.K. (1993). MKP-1 (3CH1-34), an immediate early gene product, is a dual specificity phosphatase that dephosphorylates MAP kinase *in vivo*. *Cell* **75**, 487–493.
15. Zhang, F., Strand, S., Robbins, D., Cobb, M.H. & Goldsmith, E.J. (1994). Atomic structure of the MAP kinase ERK2 at 2.3 Å resolution. *Nature* **367**, 704–711.
16. Hanks, S.K., Quinn, A.M. & Hunter, T. (1988). The protein kinase family: conserved features and deduced phylogeny of the catalytic domains. *Science* **241**, 42–52.
17. De Bondt, H.L., Rosenblatt, J., Jancarik, J., Jones, H.D., Morgan, D.O. & Kim, S.-H. (1993). Crystal structure of cyclin-dependent kinase 2. *Nature* **363**, 595–602.
18. Knighton, D.R., *et al.*, & Sowadski, J.M. (1991). Crystal structure of the catalytic subunit of cyclic adenosine monophosphate-dependent protein kinase. *Science* **253**, 407–413.
19. Taylor, S.S. & Radzio-Andzelm, E. (1994). Three protein kinase structures define a common motif. *Structure* **2**, 345–355.
20. Knighton, D.R., Zheng, J., Ten Eyck, L.F., Xuong, N.-H., Taylor, S.S. & Sowadski, J.M. (1991). Structure of a peptide inhibitor bound to the catalytic subunit of cyclic adenosine monophosphate-dependent protein kinase. *Science* **253**, 414–420.
21. Dao-Pin, S., Anderson, D.E., Baase, W.A., Dahlquist, F.W. & Matthews, B.W. (1991). Structural and thermodynamic consequences of burying a charged residue within the hydrophobic core of T4 lysozyme. *Biochemistry* **30**, 11521–11529.
22. Hubbard, S.J., Eisenmenger, F. & Thornton, J.M. (1994). Modeling studies of the change in conformaion required for cleavage of limited proteolytic sites. *Protein Sci.* **3**, 757–768.
23. Hurley, J.H., Dean, A.M., Thorsness, P.E., Koshland, D.E.,Jr. & Stroud, R.M. (1989). Regulation of isocitrate dehydrogenase by phosphorylation involves no long-range conformational change in the free enzyme. *J. Biol. Chem.* **265**, 3599–3602.
24. Lolis, E. & Petsko, G.A. (1990). Crystallographic analysis of the complex triosephosphate isomerase and 2-phosphoglycolate at 2.5-Å resolution: implications for catalysis. *Biochemistry* **29**, 6619–6625.
25. Sprang, S.R., Withers, S.G., Goldsmith, E.J., Fletterick, R.J. & Madsen, N.B. (1991). Structural basis for the activation of glycogen phosphorylase b by adenosine monophosphate. *Science* **254**, 1367–1371.
26. Zhang, F., Robbins, D.J., Cobb, M.H. & Goldsmith, E.J. (1993). Crystallization and preliminary X-ray studies of extracellular signal-regulated kinase-2/MAP kinase with an incorporated His-tag. *J. Mol. Biol.* **233**, 550–552.
27. Steigemann, W. (1989). PROTEIN: a program system for the crystal structure analysis of proteins. Martinsried vei Muenchen, FRG.
28. Brünger, A.T., Kuriyan, J. & Karplus, M. (1987). Crystallographic R factor refinement by molecular dynamics. *Science* **235**, 458–460.
29. Jones, T.A., Zou, J.-Y. & Cowan, S.W. (1991). Improved methods for building protein models in electron density maps and the location of errors in these models. *Acta Crystallogr. A* **47**,110–119.
30. Jones, T.A. (1978). A graphics model building and refinement system for macromolecules. *J. Appl. Crystallogr.* **11**, 268–272.
31. Morris, A.L., MacArthur, M.W., Hutchinson, E.G. & Thornton, J.M. (1992). Stereochemical quality of protein structure coordinates. *Proteins*, **12**, 345–364.
32. Laskowski, R.A., MacArthur, M.W., Moss, D.S. & Thornton, J.M. (1993). PROCHECK: a program to check the stereochemical quality of protein structure. *J. Appl. Crystallogr.* **26**, 283–291.
33. Engh, R.A. & Huber, R. (1991). Accurate bond and angle parameters for X-ray protein structure refinement. *Acta Crystallogr. A* **47**, 392–400.
34. Kraulis, P.J. (1991). MOLSCRIPT: a program to produce both detailed and schematic plots of protein structures. *J. Appl. Crystallogr.* **24**, 946–950.

Received: **11 Jan 1995**. Accepted: **23 Jan 1995**.